DEM SLOPE- FAILURE ANALYSIS OF THE MINAMI- ASO / TATENO AREA DURING THE 2016 KUMAMOTO EARTHQUAKES

K. ESAKI[1], H. AKAGI[1], T. KIRIYAMA[2], AND K. SATO[1]

[1] Waseda University, Department of Civil and Environmental Engineering
58-205, 3-4-1, Ohkubo, Shinjuku-ku, Tokyo, 169-8555, Japan
e-mail :esakikoichi@akane.waseda.jp, web page :
https ://www.f.waseda.jp/akagi/index_e.html

[2] Shimizu Corporation, Institute of Technology
3-4-17, Etchujima, Koto-ku, Tokyo, 135-0044, Japan
e-mail :kiriyama@shimz.co.jp, web page : https ://www.shimz.co.jp

Key words: Discrete Element Method, Kumamoto earthquakes

Abstract. The Kumamoto earthquakes, which occurred on April 16, 2016, included deep large-scale landslides in the Minami-Aso village / Tateno area; the Aso Bridge collapsed completely because of this slope failure. Aso Bridge is considered to have collapsed for various reasons, e.g., fault displacements, earthquake accelerations, and landslide sediment depositions on the bridge. In this study, the possibility of landslide-sediment depositions on the bridge was assessed as a reason for the bridge collapse using the discrete element method (DEM), and the landslides at Aso Bridge were reproduced. An experiment and analysis were conducted on the large deformation of aluminum-bar laminated ground with wall movement, to confirm the applicability of DEM to large ground-deformation problems. Next, the Aso Bridge slope-failure analysis was carried out, based on different analysis conditions, and the sediment distribution was compared with field observation results from qualitative and quantitative viewpoints. It was concluded that sediment deposition on the bridge was not a cause of the Aso Bridge failure.

1 INTRODUCTION

In recent years, concerns have been growing about geohazards triggered by earthquakes and heavy rainfall in Japan. Geohazards, e.g., slope failures and landslides, have caused heavy damage to social infrastructures. For example, the 2016 Kumamoto earthquakes that occurred on April 16, 2016, caused slope failures, landslides, and debris flow, mainly around the Aso area, and did considerable damage. Particularly, deep large-scale landslides occurred in the Minami-Aso village / Tateno area, and the Aso Bridge collapsed completely by this slope failure.

To minimize the risk of such damage, it is desirable to understand the ground-collapse process, scale, and range. However, large ground-deformation problems that range more than tens of meters have mainly been based on case studies, e.g., literature surveys and ground surveys. Along with these investigations, it is necessary to simulate the destruction process using numerical analyses, and the analyses should be evaluated using practical engineering or a physical evaluation.

The Aso Bridge might have collapsed for various reasons, e.g., fault displacements, earthquake accelerations, and landslide sediment depositions on the bridge. The definitive causes of the bridge collapse have not been determined. In this study, the possibility of landslide-sediment depositions on the bridge is assessed as a cause of the bridge collapse, using numerical analyses and reproducing the landslides at the Aso Bridge.

Finite element methods are used in engineering to evaluate the mechanical behavior of continua. However, in these methods, the mesh collapses when the ground deforms intensively in landslide simulations. Therefore, in this research, the discrete element method (DEM), which is a numerical analysis method of discrete bodies, is adopted as an analysis method. DEM was developed by Cundall [6] as a method of analyzing ground discontinuities. The applicability of the numerical analysis was evaluated from the viewpoint of large geomaterial deformations.

In this paper, an Aso Bridge slope-failure analysis is conducted. Based on Geographical Survey Institute (GSI) reports and elevation data, a 2D slope model was created of the area before the earthquake occurred. The collapse analysis was based on different analysis conditions, and the sediment distribution was compared from the qualitative and quantitative viewpoints.

2 KUMAMOTO EARTHQUAKES AND ASO BRIDGE SLOPE FAILURE

2.1 Kumamoto earthquakes in 2016

A 6.5-magnitude earthquake occurred at 9:26 pm on April 14, 2016, at a depth of about 10 km, with the Kumamoto area as the hypocenter. A seismic intensity of 7 was recorded in Mashikimachi town, Kumamoto. Then, at 1:25 am on April 16, a 7.3-magnitude earthquake occurred at a depth of about 10 km, again with the Kumamoto area as the epicenter. A seismic intensity of 7 was recorded in Mashikimachi town. The Japan Meteorological Agency identified the first as a foreshock and the second as the main earthquake.

In the foreshock on April 14, the Takano-Shirahata section of the Hinagu fault zone moved. The focal mechanism was a lateral-slip fault type with a tension axis in the north-northwest–south-southeast direction. The hypocenter fault, estimated from the aftershock distribution and focal mechanism of the earthquake, was a right-lateral slip fault extending in the north-northeast–south-southwest directions.

In the main shock on April 16, the Futagawa fault in the Futagawa fault zone moved, and the focal mechanism was a lateral-slip fault type with a tension axis in the north–south direction. The hypocenter fault estimated from the aftershock distribution and the focal mechanism of the earthquake was a right-lateral slip fault extending in the northeast–southwest direction, which included normal fault components. This Kumamoto earthquake caused construction-site runoff, river-embankment settlements, ground settlements in Aso Caldera, etc. In addition, many slope failures occurred in the Kumamoto area, including a major landslide that caused the Aso Bridge to collapse.

2.2 Slope failure of Minami Aso Tateno area

The Minami-Aso / Tateno area is located at the outer edge of the Aso Caldera, which is at the northeast end of the Futagawa fault. The eastern slope of the mountain collapsed (755.8 (m) above sea level); it is part of the Aso Caldera outer-ring mountain near Minami-Aso / Tateno.

The slope collapsed from near the top; National Road No. 57 and the main JR Hohi railway line were buried, and soil flowed into the Kurokawa River. The scale of the landslides in the Minami-Aso / Tateno area, shown in Figure 1, is estimated to be about 700 (m) in length, 200 (m) in width, 25 (m) in maximum depth, and about 500,000 (m^3) in landslide material.

The collapse range includes the JR Hohi main line, Route 57, and Route 325, which crosses the Aso Bridge over the Kurokawa River. The center of the sediment-inflow range to the river section was slightly offset from the Aso Bridge, and sediment flowed into the upper stream of the Kurokawa River. Geologically, the surface material is volcanic-ash clay (black and red) and the bedrock consists of hard andesite and semi-soft pyroclastic rock, belonging to the pre-Aso volcanic rocks. In addition, the hard andesite was confirmed to have developed fractures. The upper end of the slope was about 35 degrees steep, and the lower part was a low-gradient slope, around 15 degrees, and used as a field.

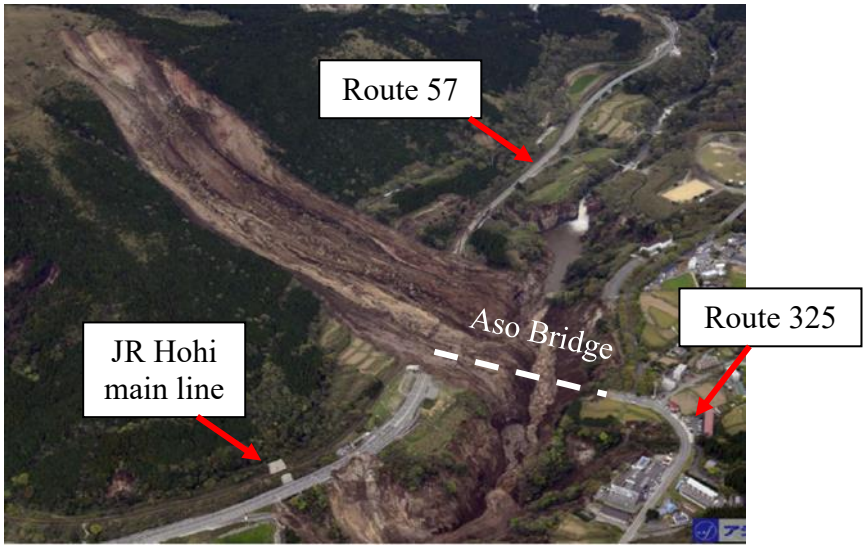

Figure 1: Slope failure of Minami Aso Tateno area [1]

3 LARGE DEFORMATION OF ALUMINUM- BAR LAMINATED GROUND WITH WALL MOVEMENT

The Aso Bridge slope was a large-scale slope failure. Thus, in this paper, the authors adopt a discrete element method (DEM) suitable for large ground-deformation analyses as a numerical analysis method. It was necessary to confirm the applicability of the DEM coded by the authors to large deformation problems. The applicability was shown by carrying out deformation experiments on aluminum-bar laminated ground with wall movement—which is a large ground-deformation problem—and comparing the experimental results with the analysis results.

3.1 Experimental apparatus and procedure

The retaining-wall test setup consists of a retaining wall and aluminum-bar laminated ground, which simulates the ground behind the retaining wall. The retaining wall is made of a rigid brass material with a height of 200 (mm), a width of 10 (mm) and a depth of 50 (mm); it can

be controlled by a handle to a horizontal displacement of 95 (mm) in the active-earth-pressure direction.

The experimental procedure is as follows. First, 200 (mm) × 50 (mm) aluminum bars are stacked. During the ground preparation, mark points for evaluating the deformation shapes are installed in the ground at 10 (mm) intervals in length and width. The ground is tightly packed, and the aluminum bars are laid as densely as possible. The aluminum bar is 50 (mm) in length, 1.6 (mm) in diameter, and 3 (mm) in circular cross section. The aluminum bars were prepared by mixing aluminum bars at a mass ratio of 2:1.

Figure 2 shows the arrangement of the retaining wall and the aluminum-bar laminated ground before the experiment. After the model ground was prepared, the retaining wall was horizontally displaced to 95 (mm) at a speed of 2 (mm/min) in the active-earth-pressure direction. The state of the experiment at that time was shot by a camera from the front of the device. From the captured video, the mark points were connected to confirm the deformation shape of the aluminum-bar laminated ground.

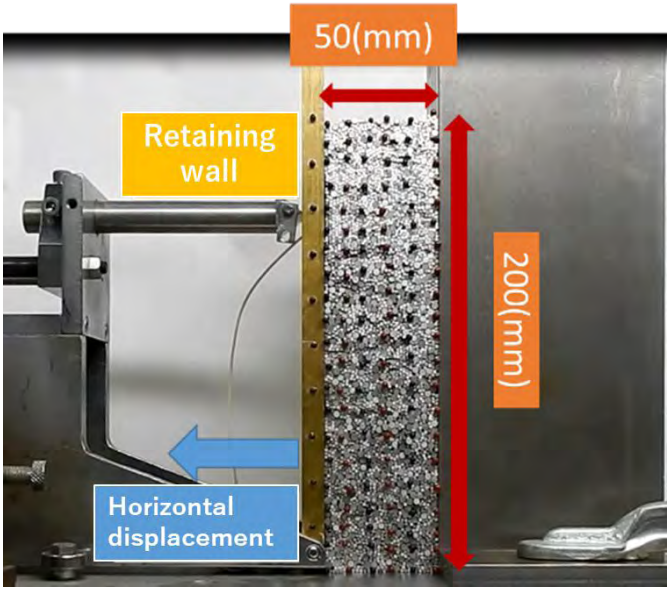

Figure 2: Retaining wall and aluminum- bar laminated ground before deformation

3.2 Analysis conditions and procedure

The DEM numerical analysis was conducted under the conditions shown in Table 1. The normal stiffness, viscous damping constant, local damping constant, and constant by which the rotational stiffness was multiplied were determined by trial calculation, considering the calculation stability. The shear stiffness was determined by introducing a reduction rate of 0.25 to the normal stiffness. The friction angle between aluminum-bar particles was shown to be 16 (°) by Matsuoka [2]. The internal friction angle was 23.5 (°) when the direct-shear test of the aluminum-bar laminated ground was conducted in previous studies [3].

In this experiment, it can be expected that the friction angle between particles will be 16 (°) or more because the friction angle between the particles changes as the granular soil changes, depending on the particles' stress state. Considering the above, the friction angle between the particles under analysis was set to 20 (°) (coefficient of friction $\mu = 0.36$). To prepare the ground

for analysis, the particles were filled using a gravity-packing method. After filling, the retaining wall was displaced at a speed of 5 (mm/s) in the active-earth-pressure direction to a displacement of 95 (mm) on analysis. The behavior of the granular material was then confirmed by visualizing. As in the experiment, mark points were installed in the ground at 10 (mm) intervals in length and width, and connected to confirm the deformation shape of the aluminum-bar laminate ground.

Table 1: Physical property values in DEM

Variable	*Unit*	Value
Integration time interval Δt	*s*	0.000002
Particle density *d*	g/cm^3	2.7
Normal stiffness k_n	*N/m*	20000000
Shear stiffness k_s	*N/m*	5000000
Viscous damping constant *h*	-	0.05
Local dumping constant α	-	0.12
Coefficient of friction μ	-	0.36
Constant- k_r by which the rotational stiffness is multiplied	-	300000

3.3 Experimental and analysis results

The analysis results were compared with experimental results. The red frame in Figure 3 is the outline of the aluminum-bar laminated ground. From the deformed figure in Figure 3, it is clear that the experimental and the analytical results correspond well at displacements of 65 (mm), 80 (mm), and 95 (mm). On the other hand, at displacements from 5 (mm) to 35 (mm), it is clear that the outline of the granular soils in the analysis result is smaller than the outline of the experimental result. This is due to the use of gravity packing to prepare the ground for analysis.

When the ground was prepared for the experiment, the aluminum bars were laid as densely as possible; however, in the gravity-packing method, the particles were not packed as densely as in the experiment. With the movement of the retaining wall, the ground volume tended to expand in the experiment and contract in the analysis. The effects of the volume expansion and contraction decreased with the movement of the retaining wall, and the outline of the experimental results and the analytical results were gradually approximated for displacements of 80 (mm) and 95 (mm), whose deformations were large.

From these results, the authors qualitatively evaluated and demonstrated the applicability of DEM to large deformation problems.

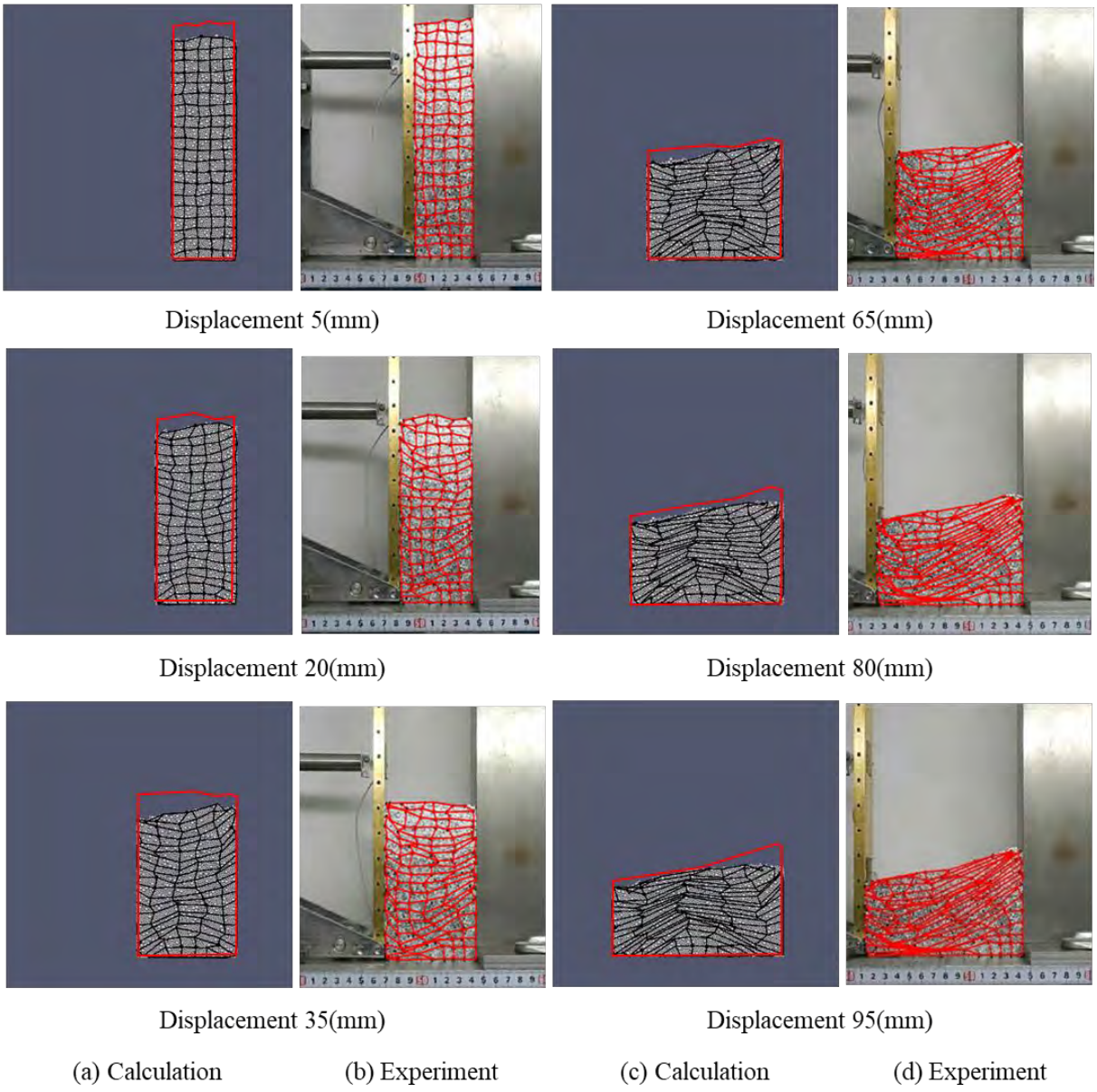

Figure 3: Comparison of deformation between analysis and experiment

4 NUMERICAL ANALYSIS OF ASO BRIDGE SLOPE FAILURE

4.1 Creation of analysis model

The field-survey report about the slope failure that occurred in the Minami-Aso / Tateno area [1] confirmed that part of the soil that collapsed on the west side of the Aso Caldera wall, which is at the top of the slope, was deposited in the middle of the slope, and most of the remainder flowed into the Kurokawa River. The scale of the collapse was about 700 (m) in length, 200 (m) in maximum width, 25 (m) in maximum depth, and 500,000 (m^3) in landslide material.

Based on the report and elevation data from the Geographical Survey Institute (GSI), a 3D

CAD model of before the earthquake occurred was created, and the flow range was estimated by comparing aerial photographs from after the earthquake with the 3D CAD model (Figure 4). Under this condition, a two-dimensional cross section in the longitudinal direction was extracted. In this section, based on the report data [3], the slope width and depth were set to 200 (m) and 25 (m), respectively (Figure 5), and the ground-surface shape was estimated, assuming the arc slip surface. A two-dimensional slope was determined (Figure 6), which approximated the estimated soil volume of 500,000 (m^3) by calculating the total soil volume on the arc-slip surface by adding the area of the small trapezoid from the slope coordinates and the coordinates of the set arc lower limit. This is the surface shape of the 2D slope-failure model used for the DEM analysis.

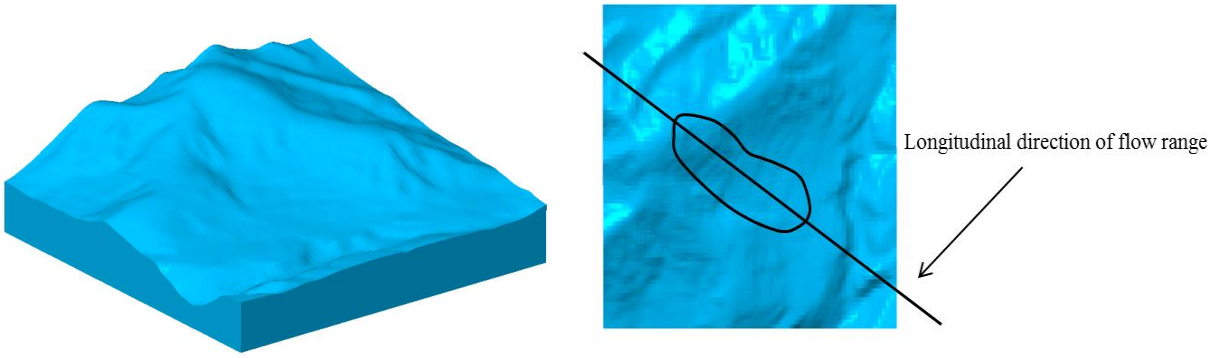

Figure 4: 3D CAD before the Kumamoto earthquake and Estimation of flow range

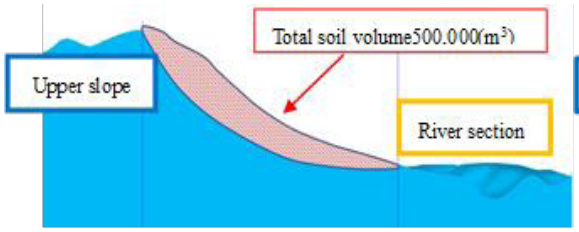

Figure 5: Estimation of slope shape by arc slip

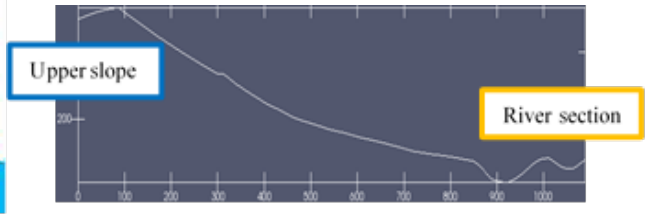

Figure 6: Surface shape in analysis model

4.2 Determination of parameters and case studies

First, 0.25 (m)-diameter particles were packed using gravity packing into the collapse area in the determined ground-surface shape. A slope-failure analysis was performed, on the assumption that the filled particles reached downstream in 100 (s) by their own weight.

The physical properties used for the DEM analysis are shown in Table 2. The viscosity coefficient and the local damping constant were determined by parametric studies, considering the stability of the calculation. In this paper, the deposition shapes and flow tendency are compared for three cases by considering the cohesion force and coefficient of friction during the slope failure. The DEM analysis was performed for large (Case 1), intermediate (Case 2), and small values (Case 3). Table 3 shows the physical property values of the three cases. The analysis results were compared, and the influence of the physical property values during the slope failure in the DEM analysis was investigated.

Table 2: Physical property values used for DEM analysis

Variablle	Unit	Value
Integration time interval Δt	s	0.00002
Particle density d	g/cm^3	1.6
Normal stiffness (between particles)k_n	N/m	1.0×10^7
Shear stiffness (between particles) k_s	N/m	2.5×10^6
Normal stiffness (between particle walls)k'_n	N/m	1.0×10^8
Shear stiffness (between particle walls) k'_s	N/m	2.5×10^7
Viscosity coefficient h	$N \cdot s/m$	1.0
Local dumping constant α	-	0.05

Table 3: Physical property values of three cases

Variable	*Unit*	Case1	Case2	Case3
Coefficient of friction μ	-	0.58	0.27	0.18
Cohesive force k_r	*kPa*	10	5	2

4.3 Discussions

The analysis results of Cases 1 through 3 are compared. Figure 7 shows the initial deposition shape of the particles in the DEM analysis. The particles placed at the upper part of the slope flow onto the slope with the passage of time, are deposited on the middle part of the slope, and flow into the river. The DEM simulation results confirmed that the flow tendency, e.g., the speed in reaching the river area, and the shape of the deposition differ depending on the coefficient of friction and the cohesive force. Particularly, the greater the cohesion force and coefficient of friction, the lower the flowability, and the particles tend to stay upstream of the slope.

This tendency is evaluated by the difference in sediment distribution. As shown in Figure 8, the slope was divided into four areas (upper section, middle section 1, middle section 2, and river section), and Figure 9 shows the sediment distribution in each case. It was confirmed that the sediment distribution on the slope is different in each case.

In Case 1, the sediment flowed slowly, and most of it was deposited in the upper section and middle section 1. At 100 (s), 270,000 (m^3) were deposited in the upper section, 220,000 (m^3) in middle section 1, and 996 (m^3) flowed into the river section.

In Case 2, the sediment passed through the upper section by 40 (s), and then was gradually deposited in the middle section. At 100 (s), about 350,000 (m^3) were deposited in the upper section, 290,000 (m^3) in middle section 1, 170,000 (m^3) in middle section 2, and 3,675 (m^3) flowed into the river section.

In Case 3, the sediment flowed quickly, and most sediment passed through the upper section by 20 (s) and converged to the final sediment-deposition state by 50 (s). About 113,000 (m^3) of sediment was deposited in middle section 2, and the rest of the sediment, 380,000 (m^3), flowed into the river section.

From these results, it was confirmed that the speed of the sediment arriving in the river and the deposition shape differed, depending on the coefficient of friction and the cohesion force. The disaster report [1] confirmed that, in the actual slope failure in the Minami-Aso / Tateno area, the majority (about 500,000 m^3) of the sediment that collapsed in the upper section was deposited in middle section 2 and flowed into the river section. Therefore, the authors judged Case 3 to be an appropriate analysis result, considering the sediment distribution.

Regarding the inflow sediment around the Aso Bridge, it was confirmed that the majority of the inflow sediment flowed into the upstream side of the Kurokawa River. Therefore, in Case 3, not all of the 380,000 (m^3) of sediment that flowed into the river section was deposited on the Aso Bridge. In other words, the sediment deposition on the Aso Bridge was relatively modest. Estimating from the analysis results, it was concluded that sediment deposition was unlikely to be the main reason for the collapse of the Aso Bridge.

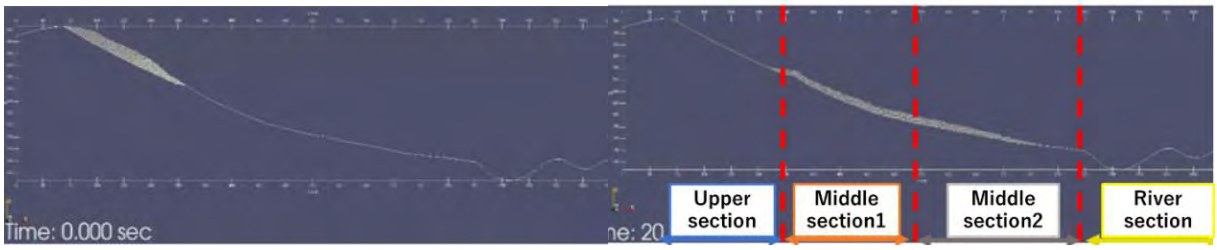

Figure 7: Initial deposition shape of DEM analysis

Figure 8: Division of slope area

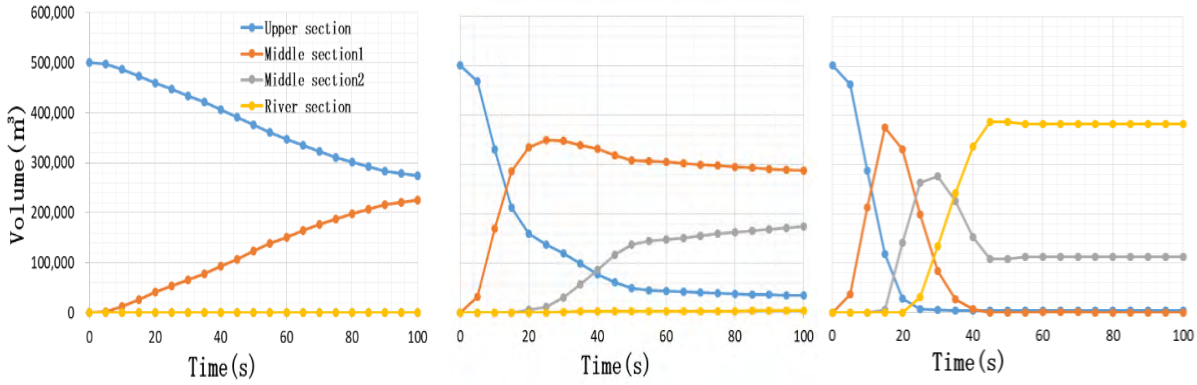

Figure 9: Sediment volume change over time at each section

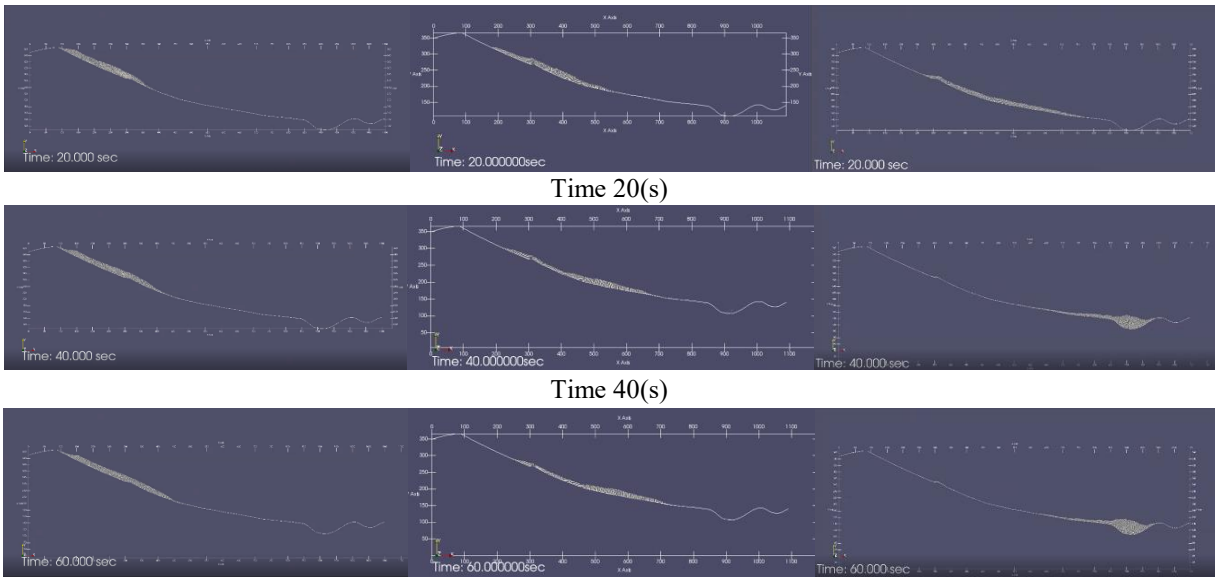

Figure 10: Sediment distribution situations

5 CONCLUSION

In this paper, the slope failure in the Minami-Aso / Tateno area during the 2016 Kumamoto earthquakes was analyzed using DEM. The deposition shape and flow tendency, due to the difference in the coefficient of friction and the adhesion force failure, were confirmed, and these tendencies were quantitatively compared and considered, regarding the difference in sediment distribution. From the final sediment deposition on the slope and the inflow to the river, Case 3, with a relatively low coefficient of friction and cohesion force, was judged to be a highly reproducible analysis result. From the estimated sediment distribution amount, the authors concluded that sediment deposition on the bridge was not a cause of the Aso Bridge failure.

A future issue is the re-examination of the sediment arrival speed in Case 3. Case 3 converges to the final deposition shape at 50 (s); however, in the actual slope failure, the sediment-flow velocity was slow. It is necessary to reexamine the viscosity coefficient and the local damping constant related to the analytical stability calculation.

REFERENCES

[1] Earth and sand disaster emergency investigation team pertaining to the 2016 Kumamoto earthquake (2016). Emergency investigation report on earth and sand disaster due to the 2016 Kumamoto earthquake, Japan Society of Erosion Control Engineering, 15–24 (in Japanese).

[2] 2016 Kumamoto Earthquake Geotechnical Disaster Investigation Team (2017). Field survey report on slope disaster caused by the 2016 Kumamoto earthquake, The Japanese Geotechnical Society (in Japanese).

[3] H. Matsuoka, K. Saiki (1992). A Measurement Method of Interparticle Friction Angle (φ_μ) of Two-Dimensional Granular Body (Round Bar), The 27th Geotechnical Engineering Conference, 579–580 (in Japanese).
[4] ITASCA (2002). PFC2D Online Manual, Table of Contents—Theory and Background—Section 1: General Formulation.
[5] Structure and landslide disaster investigation team (2016). 2016 Kumamoto earthquake survey report, International Research Institute of Disaster Science (in Japanese).
[6] P. Cundall (1987). Distinct element models of rock and soil structure, Analytical and Computational Methods in Engineering Rock Mechanics, Ch. 4, 129–163. E.T. Brown, ed., London: Allen & Unwin.
[7] K. Imada, H. Akagi, A. Saito, T. Kiriyama (2018). Slope Failure Analysis of Minami Aso Tateno District due to Kumamoto Earthquake Using DEM, The 73rd Japan Society of Civil Engineers Conference, 589–590 (in Japanese).
[8] K. Esaki, H. Akagi, A. Saito, T. Kiriyama (2018). Large deformation analysis of aluminum bar model ground with wall movement by using Discrete Element Method, The 73rd Japan Society of Civil Engineers Conference, 743–744 (in Japanese).